Volume 24, No 4 | International Journal of Radiation Research, October 2026

Values of multimodal magnetic resonance imaging (MRI) for identification and diagnosis of demyelinating pseudotumor (DPT) and glioma

Y. Chen[1#], L. Wei[1#], C. Zheng[1], S. Zhan[1], S. Chen[2*], X. Yang[3,4*]

[1]*Department of Radiology, Zhangzhou Affiliated Hospital of Fujian Medical University, Zhangzhou, 363000, Fujian Province, China*
[2]*Department of Human Anatomy, Fujian Medical University, Fuzhou,350000, Fujian Province, China*
[3]*Department of Ultrasound Medicine, Zhangzhou Affiliated Hospital of Fujian Medical University, Zhangzhou, 363000, Fujian Province, China*
[4]*Department of Ultrasound Medicine, Peking Union Medical College, Beijing,100005, China*

► ***Original article***

***Corresponding author:**
Xiao Yang, Shaoqiang Chen, M.D.
***E-mail:** yangxiao1@pumch.cn, 1574523258@qq.com*

Received: May 2026
Final revised: July 2026
Accepted: July 2026

Int. J. Radiat. Res., October 2026; 24(4): 1017-1021

DOI: 10.61186/ijrr.24.4.11

Keywords: *Demyelinating pseudotumor, tumor-like demyelinating lesions, glioma, magnetic resonance imaging, multimodal MRI.*

#These authors made equal contribution to the work.

ABSTRACT

Background: This to research aims to evaluate values of conventional MRI and multimodal MRI for identification and diagnosis of tumor-like demyelinating lesions (TDL), also referred to as demyelinating pseudotumor (DPT), and glioma, with a focus on imaging-based differentiation between the two conditions. ***Materials and Methods:*** Conventional MRI sequences including T1-weighted imaging (T1WI), T2-weighted imaging (T2WI), fluid-attenuated inversion recovery (FLAIR), and contrast-enhanced T1WI, as well as multimodal MRI sequences including diffusion-weighted imaging (DWI), susceptibility-weighted imaging (SWI), magnetic resonance spectroscopy (MRS), and dynamic susceptibility contrast MRI (DSC-MRI), were retrospectively analyzed in 61 patients with pathologically confirmed TDL and 66 patients with glioma. ***Results:*** On conventional MRI, glioma lesions were significantly larger than TDL lesions (mean diameter 41.3 mm vs. 24.4 mm, $p<0.001$), more frequently involved the cerebral cortex (80.3% vs. 31.1%), and exhibited greater perilesional edema and mass effect ($p<0.001$). TDL lesions more commonly demonstrated open-ring enhancement (54.1% vs. 19.7%, $p<0.001$) and a central vein sign on SWI (27.9% vs. 7.6%, $p<0.05$). MRS revealed significantly higher choline (Cho)/N-acetylaspartate (NAA) and Cho/creatine (Cr) ratios and lower NAA/Cr ratios in glioma compared to TDL ($p<0.05$). DSC-MRI demonstrated hyperperfusion in all examined glioma lesions (9/9) versus hypoperfusion in the majority of TDL lesions (7/8, $p<0.001$). ***Conclusion:*** The combination of conventional MRI and multimodal MRI sequences-particularly open-ring enhancement on contrast-enhanced T1WI, the central vein sign on SWI, metabolite ratios (Cho/NAA, Cho/Cr, NAA/Cr) on MRS, and perfusion patterns on DSC-MRI-provides significant discriminative value for differentiating TDL from glioma, and is superior to reliance on conventional MRI alone.

INTRODUCTION

Tumor-like demyelinating lesions (TDL), also known as demyelinating pseudotumor (DPT) or tumefactive demyelinating lesions, represent a rare category within the spectrum of inflammatory demyelinating conditions affecting the central nervous system (CNS) [1]. Characteristically, these lesions exceed 20 mm in diameter and can present with mass effect and surrounding edema of varying severity. Additionally, emerging research suggests potential links of TDL with other neuroinflammatory disorders, such as neuromyelitis optica spectrum disorder (NMOSD) and myelin oligodendrocyte glycoprotein antibody-associated disease (MOGAD) [2]. Clinically, TDL often resembles CNS tumors, and imaging findings may include prominent mass effect, extensive perilesional edema, and ring enhancement-features commonly seen in malignant CNS tumors [3]. Consequently, TDL is frequently misdiagnosed as glioma on imaging, leading to unnecessary surgical interventions.

The differentiation of TDL from glioma remains a significant clinical challenge. Gliomas are the most prevalent primary brain tumors, spanning WHO grades I-IV, and carry markedly different prognoses and treatment strategies compared to TDL [4]. Conventional MRI features such as lesion morphology, enhancement patterns, and perilesional edema have been proposed as discriminating criteria; however, overlap between TDL and high-grade glioma on conventional imaging is substantial [5, 6]. Advanced multimodal MRI techniques, including DWI, which reflects tissue cellularity through water

[Downloaded from ijrr.com on 2026-11-08]

[DOI: 10.61186/ijrr.24.4.11]

diffusion restriction [7]; SWI, which can reveal paramagnetic susceptibility changes and venous structures [8]; MRS, which provides metabolic profiling of brain lesions [9]; and DSC-MRI, which quantifies lesion hemodynamics [10], have shown promise in distinguishing inflammatory from neoplastic lesions. Nevertheless, systematic studies integrating all four modalities in a direct TDL-versus-glioma comparison with a sufficiently large, pathologically confirmed cohort remain scarce [11, 12].

Current research on TDL primarily relies on conventional MRI, whereas multimodal MRI approaches remain underexplored in the context of TDL versus glioma differentiation. The novelty of the present study lies in its comprehensive, multimodal MRI framework- integrating conventional sequences with DWI, SWI, MRS, and DSC-MRI- applied to a relatively large cohort of pathologically confirmed TDL (n=61) and glioma (n=66) cases. The aim is to establish objective, multimodal imaging criteria to guide clinical differentiation of TDL from glioma without sole reliance on histopathological biopsy.

MATERIALS AND METHODS

General data

Clinical and imaging data of 61 TDL patients and 66 glioma patients (WHO grades I–IV) admitted to our hospital between 2018 and 2023 were collected. Inclusion criteria: ① complete medical records and pathological data; ② clear and intact imaging; ③ TDL lesions >2mm in diameter; ④ no concurrent intracranial space-occupying lesions.

Examination methods

MRI data were obtained using a 3.0 T MRI system with an 8-channel head coil (Philips Ingenia, Philips Healthcare, Best, the Netherlands). Contrast-enhanced imaging was performed using gadopentetate dimeglumine (Magnevist®, Bayer Schering Pharma, Berlin, Germany) at a dose of 0.1 mmol/kg body weight, administered intravenously. Image post-processing was performed using dedicated software integrated in the Philips IntelliSpace Portal workstation (Philips Healthcare, Best, the Netherlands).

The MRI scanning protocol comprised the following sequences:

① Conventional MRI sequences:

T1WI: repetition time (TR)/echo time (TE) = 450/10 ms; slice thickness = 5 mm; field of view (FOV) = 230×230 mm; matrix = 256×256.

T2WI: TR/TE = 4000/90 ms; slice thickness = 5 mm; FOV = 230×230 mm; matrix = 256×256.

FLAIR: TR/TE/inversion time (TI) = 9000/120/2500 ms; slice thickness = 5 mm; FOV = 230×230 mm; matrix = 256×256.

Contrast-enhanced T1WI: same parameters as T1WI above, acquired in axial, coronal, and sagittal planes following intravenous contrast administration.

② Multimodal MRI sequences:

DWI: echo-planar imaging (EPI) sequence; TR/TE = 4000/70 ms; b-values = 0 and 1000 s/mm^2; slice thickness = 5 mm; FOV = 230×230 mm; matrix = 128×128. Apparent diffusion coefficient (ADC) maps were automatically generated.

SWI: TR/TE = 19/27 ms; flip angle = 15°; slice thickness = 2 mm; FOV = 230×230 mm; matrix = 384×384. Minimum intensity projection (mIP) reconstructions over 4 contiguous slices were generated.

MRS: single-voxel point-resolved spectroscopy (PRESS) sequence; TR/TE = 2000/35 ms; voxel size = 15×15×15 mm^3; number of averages = 128. Metabolite ratios including Cho/NAA, Cho/Cr, and NAA/Cr were calculated. MRS was performed in 12 TDL patients and 42 glioma patients.

DSC-MRI: gradient-echo EPI sequence; TR/TE = 1500/30 ms; slice thickness = 5 mm; FOV = 230×230 mm; matrix = 128×128; 50 dynamic phases acquired during bolus injection of gadopentetate dimeglumine (0.1 mmol/kg, injection rate 4 mL/s). Relative cerebral blood volume (rCBV) maps were generated using dedicated perfusion analysis software. DSC-MRI was performed in 8 TDL patients and 9 glioma patients.

Image analysis

All statistical evaluations were performed with SPSS version 26.0 (IBM Corp., Armonk, NY, USA). Continuous data conforming to a normal distribution were compared using the independent samples t-test. The rank-sum test was applied to compare non-normally distributed continuous data. Categorical variables were analyzed with Pearson's chi-square test, whereas Fisher's exact test was adopted in cases where more than 25% of the cells had an expected count below 5. A p-value of <0.05 was considered statistically significant.

Statistical analysis

All statistical evaluations were performed with SPSS 26.0 software. Continuous data conforming to a normal distribution were compared using the independent samples t-test. The rank-sum test was applied to compare non-normally distributed count data. Categorical variables were analyzed with Pearson’s chi-square test, whereas Fisher’s exact test was adopted in cases where more than 25% of the cells had an expected count below 5.

RESULTS

General clinical data

The mean age of TDL patients (37.1±13.41) was younger than that of glioma patients (53.2±18.82),

[Downloaded from ijrr.com on 2026-11-08]

[DOI: 10.61186/ijrr.24.4.11]

and the proportion of female patients was higher in TDL than in glioma (P=0.015). TDL more frequently presented with subacute/chronic onset (≥4 weeks), and patients with TDL had higher rates of ataxia, sensory disturbances, and motor dysfunction compared to glioma patients (P<0.001). Conversely, glioma patients had a higher proportion of acute onset (<4 weeks) and exhibited greater frequencies of epilepsy and headache than TDL patients (P<0.01). Only 3.3% of TDL patients presented with epilepsy (table 1).

Table 1. General clinical data of the two groups.

	Tumor-Like Demyelinating Lesions (TDL)	Glioma	P-value
Number of cases	61	66	
Age	37.4±13.41	53.2±18.82	<0.001
gender			0.015
Male	22(36.1%)	38(57.6%)	
Female	39(63.9%)	28(42.4%)	
Acuteness of onset			0.016
Acute phase	23(37.7%)	39(59.1%)	
Subacute/chronic phase	38(62.3%)	27(40.9%)	
Epilepsy	2(3.3%)	12(18.2%)	0.007
Ataxia	30(49.2%)	3(4.5%)	<0.001
Paresthesia disorder	17(27.9%)	2(3.0%)	<0.001
Dyskinesia	35(57.4%)	15(22.7%)	<0.001
Headache	10(16.4%)	41(62.1%)	<0.001
Visual disturbance	9(14.8%)	4(6.1%)	0.106

MRI image analysis results

Lesion location, size, and perilesional involvement

Both TDL and glioma lesions were predominantly located in the supratentorial region (above the tentorium cerebelli). TDL lesions were more frequently located in the infratentorial region (26.2%) compared to gliomas (4.6%) (P=0.003). The mean maximum diameter of TDL lesions was smaller than that of glioma lesions (P<0.001). Based on the size of the perilesional edema belt, edema severity was categorized [13]: mild edema (<1 cm) and moderate-to-severe edema (>1 cm). TDL lesions exhibited less severe edema than glioma lesions (P<0.001). According to the degree of mass effect on surrounding tissues, the extent of space occupation was classified [13]: ① mild: disappearance of surrounding sulci; ② compression and deformation of adjacent ventricles; ③ midline shift. TDL lesions showed less severe mass effect than glioma lesions (P<0.001). Gliomas involved the cerebral cortex at a higher rate (80.3%) than TDL lesions (31.1%).

MRI features of lesions in both groups

No statistically significant disparity in the edge-restricted diffusion pattern was noted on DWI between the two groups (P=0.461); both could present as diffuse restriction, open-ring restriction, or closed-ring restriction. However, their enhancement patterns differed: TDL lesions showed open-ring enhancement in a higher proportion (54.1%) than gliomas (P<0.001), whereas gliomas more frequently exhibited closed-ring enhancement. By combining DWI with ADC images, 57.6% of gliomas displayed central nodular restricted diffusion, and 68.2% of lesions showed central nodular enhancement (figure 1). These two features were less common in TDL lesions than those in gliomas (P<0.001). On SWI, 27.9% of TDL patients exhibited a central venous sign (figure 2), compared with only 7.6% of glioma patients (P<0.05). Among the 12 TDL and 42 glioma cases that underwent MRS imaging, TDL lesions had lower Cho/Cr and Cho/NAA ratios than gliomas (P<0.05) and higher NAA/Cr ratios (P<0.001). For the 8 TDL and 9 glioma patients who underwent DSC-MRI, 7 TDL lesions showed low perfusion and only 1 showed high perfusion, whereas all glioma lesions exhibited high perfusion (P<0.001) (table 2).

Table 2. Comparison of imaging findings between the two groups.

	Tumor-Like Demyelinating Lesions (TDL)	Glioma	P-value
Number of cases	61	66	
Location of lesion			0.003
Supratentorial lobe	38(62.3%)	55(83.3%)	
Basal ganglia/thalamus	7(11.5%)	8(12.1%)	
Infratentorial	16(26.2%)	3(4.6%)	
Size	24.4±13.25	41.3±6.71	<0.001
Lesion boundary			0.064
Clear	35(57.4%)	27(40.9%)	
Unclear	26(42.6%)	39(59.1%)	
Degree of edema			<0.001
None/Mild	53(86.9%)	14(21.2%)	
Moderate/severe	8(13.1%)	52(78.8%)	
Place occupancy effect			<0.001
None/Mild	59(96.7%)	15(22.7%)	
Moderate/severe	2(3.3%)	51(77.3%)	
Vertical sign of lateral ventricle	36(59.0%)	19(28.8%)	<0.001
Cerebral cortical involvement	19(31.1%)	53(80.3%)	<0.001
Edge dispersion restricted mode			0.461
Unrestricted/diffusely restricted	30(49.2%)	27(40.9%)	
Closed-loop dispersion limited	9(14.8%)	8(12.1%)	
Open-loop diffuse involvement	22(36.0%)	31(47%)	
Edge enhancement form			<0.001
No enhancement/diffuse enhancement	26(42.6%)	25(37.9%)	
Closed-loop reinforcement	2(3.3%)	28(42.4%)	
Open-loop strengthening	33(54.1%)	13(19.7%)	
Central diffusion restricted	15(24.6%)	38(57.6%)	<0.001
Center reinforcement	20(32.8%)	45(68.2%)	<0.001
SWI (central venous sign)	17(27.9%)	5(7.6%)	0.003
MRS	N=12	N=42	
NAA/Cr	1.26	0.75	<0.001
Cho/Cr	1.57	2.25	0.017
Cho/NAA	1.48	3.43	<0.001
MR perfusion imaging	N=8	N=9	<0.001
Hyperperfusion	1	9	
Hypoperfusion	7	0	

[Downloaded from ijrr.com on 2026-11-08]

[DOI: 10.61186/ijrr.24.4.11]

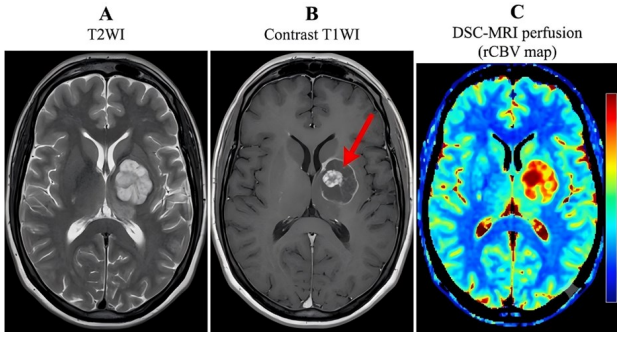


Figure 1. A 58-year-old male patient with glioma (WHO grade III). **A.** T2-weighted imaging (T2WI) shows a lobulated, slightly hyperintense lesion in the left thalamus with moderate surrounding edema. **B.** Contrast-enhanced T1-weighted imaging (T1WI) reveals a nodular enhancing focus within the lesion (red arrow), consistent with central nodular enhancement. **C.** Dynamic susceptibility contrast MRI (DSC-MRI) perfusion imaging demonstrates high perfusion (elevated relative cerebral blood volume) within the lesion, indicative of glioma-related neovascularization.

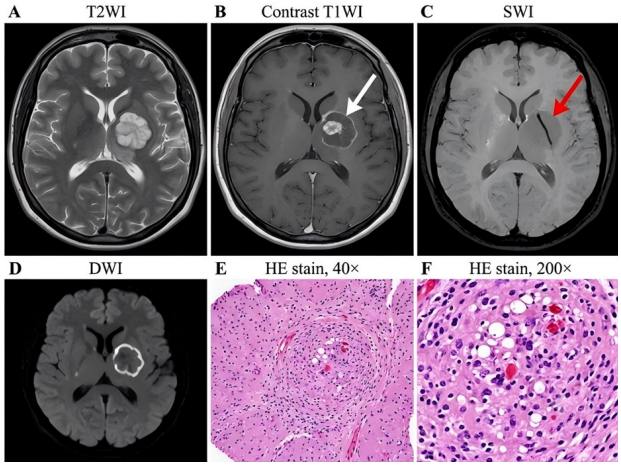


Figure 2. A 26-year-old female patient with tumor-like demyelinating lesion (TDL). **A.** T2WI shows a hyperintense lesion in the basal ganglia region, which has not involved the cerebral cortex. **B.** Contrast-enhanced T1WI reveals mild ring enhancement with an open-ring sign (white arrow), a characteristic feature of TDL. **C.** Susceptibility-weighted imaging (SWI) demonstrates a central vein within the lesion (red arrow), representing the central vein sign. D. DWI indicates open-ring restricted diffusion in the lesion. E. Pathological microscopy (hematoxylin and eosin [HE] staining, 4×10 magnification) reveals focally increased cellularity in the brain tissue with lymphocytic and plasmacytic infiltration, and focal formation of vascular lymphocytic cuffs. F. Pathological microscopy (HE staining, 20×10 magnification) shows focal interstitial hemorrhage and cellular vacuolar degeneration, confirming the demyelinating nature of the lesion.

DISCUSSION

TDL predominantly affects younger individuals, with a mean age of 37.1 years in the present cohort, in contrast to glioma patients whose mean age was 53.2 years. A higher proportion of female patients was observed in TDL, consistent with the known predilection of demyelinating diseases for women [1, 6]. French *et al.* [6] similarly reported subacute/chronic onset as a characteristic feature of TDL, and our findings align with this observation. The higher prevalence of epilepsy and headache in glioma patients is consistent with prior literature, in which seizures have been reported as a presenting feature in 20-40% of glioma cases, compared with only 3.3% in the present TDL cohort [5].

Imaging-wise, TDL lesions are generally smaller than glioma lesions-consistent with findings reported by Jeong *et al.* [7] and Yiu *et al.* [8] with a mean diameter of approximately 24.4 mm, and 26.2% of TDL lesions occur in the infratentorial region. In contrast, glioma lesions are larger, rarely involve the infratentorial region, and are more prone to involve gray matter. TDL lesions often display peripheral open-ring enhancement, which is considered a result of central vascular thrombosis-induced necrosis, while the open-ring enhancement is attributed to neovascularization at the inflammatory boundary caused by macrophage infiltration [14]. This open-ring enhancement pattern is regarded as a characteristic imaging marker of TDL and has been described as pathologically corresponding to active demyelination at the lesion periphery with relative central sparing [14]. No significant differences were observed in the annular diffuse restricted diffusion pattern on DWI between TDL and gliomas. However, in concordance with prior work [5, 8], a greater number of gliomas exhibited central diffuse restricted diffusion and central enhancement, whereas TDL rarely presented with this pattern. On SWI, 27.9% of TDL lesions showed a central vascular shadow. Studies suggest that TDL originates from the central vein and progresses peripherally, with lymphocytic infiltration around the central vein triggering inflammatory responses, demyelination, and centrifugal expansion [15]. The absence of a visible central vein in some TDL lesions may be due to insufficient MRI field strength or central venous occlusion [16]. The central vein sign has been demonstrated as a useful marker for discriminating inflammatory demyelinating lesions from other white matter pathologies, including at 3T MRI [15], supporting its utility as identified in the present study. On MRS imaging, TDL exhibited lower Cho/Cr and Cho/NAA ratios than gliomas ($p<0.05$), and higher NAA/Cr ratios than gliomas ($p<0.001$). In gliomas, elevated Cho serves as a biomarker reflecting phospholipid turnover associated with tumor cell proliferation and myelin fiber destruction [9]. In the context of demyelinating diseases, research has shown that increased Cho levels are linked to reactive astrocyte proliferation, local ischemia, and impaired mitochondrial function in neurons [17]. The reduction in NAA/Cr in glioma further reflects damage to normal neurons and neuronal loss, as previously reported [9]. Among the 9 glioma patients who underwent DSC-MRI, all showed hyperperfusion,

[Downloaded from ijrr.com on 2026-11-08]

[DOI: 10.61186/ijrr.24.4.11]

likely due to abundant immature tumor neovessels in glioma lesions-a well-recognized feature of high-grade gliomas [18]. In contrast, 7 of 8 TDL patients showed hypoperfusion, which may be attributed to microcirculatory disruption caused by extensive lymphocytic infiltration around lesion vessels [18]. The hyperperfusion observed in one TDL case might result from compensatory vasodilation and collateral circulation formation due to surrounding inflammatory reactions [10].

In summary, TDL and gliomas can be challenging to differentiate based on conventional imaging and clinical features alone. By synthesizing features from both conventional and multimodal MRI, the present work advances the comprehension of TDL and clarifies critical distinguishing features between TDL and gliomas. The multimodal approach-particularly the integration of open-ring enhancement on contrast T1WI, central vein sign on SWI, metabolite ratios on MRS, and perfusion patterns on DSC-MRI-offers incremental diagnostic value beyond conventional MRI alone. In clinical practice, when conventional MRI sequences are insufficient for diagnosing or differentiating TDL, functional magnetic resonance imaging can provide additional diagnostic information. A limitation of the present study is that MRS and DSC-MRI were not performed in all patients, resulting in smaller subgroup sizes for these modalities. Future prospective studies with larger cohorts and standardized multimodal protocols are warranted.

***Acknowledgments*:** Not applicable.

***Ethics approval and consent to participate*:** he study was conducted in accordance with the Declaration of Helsinki and approved by the Ethics Committee of Zhangzhou Affiliated Hospital of Fujian Medical University, China (Approval No.: [ZZYY-2018 -XXX]; Date of approval: [January 2018]). Informed consents were obtained from all patients.

***Consent for publication*:** Not applicable.

***Availability of data and materials*:** The datasets used and/or analyzed during the current study are available from the corresponding author on reasonable request.

Competing interests: The authors declare that they have no competing interests

Funding: The study was supported by 2025 Zhangzhou Science and Technology Plan Projects (Guiding Program) (Grant zz20250009) and 2025 Natural Science Foundation of Fujian Province (General Program) (Grant 2025J011622).

Authors' contributions: L.W. and S.Z., designed the study and drafted the manuscript. C.Z. and L.H., were responsible for the collection and analysis of the experimental data. L.W. and Y.C., revised the manuscript critically for important intellectual content. All authors read and approved the final manuscript.

AI usage declaration: No artificial intelligence tools were used in the preparation, writing, or analysis of this manuscript.

REFERENCES

1. Patriarca L, Torlone S, Ferrari F, Di Carmine C, *et al.* (2016) Is size an essential criterion to define tumefactive plaque? MR features and clinical correlation in multiple sclerosis. *Neuroradiol J,* ***29****(5): 384-389*.
2. Katsuse K, Kurihara M, Sugiyama Y, Kodama S, *et al.* (2019) Aphasic status epilepticus preceding tumefactive left hemisphere lesion in anti-MOG antibody associated disease. *Mult Scler Relat Disord,* ***27****: 91-94*.
3. Weinshenker BG (2015) Tumefactive demyelinating lesions: Characteristics of individual lesions, individual patients, or a unique disease entity? *Mult Scler,* ***21****(13): 1746-1747*.
4. Ostrom QT, Cioffi G, Waite K, Kruchko C, Barnholtz-Sloan JS (2021) CBTRUS Statistical Report: Primary Brain and Other Central Nervous System Tumors Diagnosed in the United States in 2014–2018. *Neuro Oncol,* ***23****(Suppl 2): iii1-iii105*.
5. Lin X, Yu WY, Liauw L, Chander RJ, *et al.* (2017) Clinicoradiologic features distinguish tumefactive multiple sclerosis from CNS neoplasms. *Neurol Clin Pract,* ***7****(1): 53-64*.
6. French H, Fontes-Villalba A, Maharaj M, Naidoo CSY, *et al.* (2022) Tumefactive multiple sclerosis versus high grade glioma: A diagnostic dilemma. *Surg Neurol Int,* ***13****: 146*.
7. Jeong IH, Kim SH, Hyun JW, Joung A, *et al.* (2015) Tumefactive demyelinating lesions as a first clinical event: Clinical, imaging, and follow-up observations. *J Neurol Sci,* ***358****(1-2): 118-124*.
8. Yiu EM, Laughlin S, Verhey LH, Banwell BL, Canadian Pediatric Demyelinating Disease Network (2014) Clinical and magnetic resonance imaging (MRI) distinctions between tumefactive demyelination and brain tumors in children. *J Child Neurol,* ***29****(5): 654-665*.
9. Chronaiou I, Stensjøen AL, Sjøbakk TE, Esmaeili M, Bathen TF (2014) Impacts of MR spectroscopic imaging on glioma patient management. *Acta Oncol,* ***53****(5): 580-589*.
10. Cha S, Pierce S, Knopp EA, Johnson G, *et al.* (2001) Dynamic contrast-enhanced T2*-weighted MR imaging of tumefactive demyelinating lesions. *AJNR Am J Neuroradiol,* ***22****(6): 1109-1116*.
11. Sahraian MA, Radue EW, Haller S, Kappos L (2010) Black holes in multiple sclerosis: definition, evolution, and clinical correlations. *Acta Neurol Scand,* ***122****(1): 1-8*.
12. Suthiphosuwan S, Bharatha A, Hsu CC, Hojjat SP, *et al.* (2021) Tumefactive demyelinating lesions in radiologically isolated syndrome. *AJNR Am J Neuroradiol,* ***42****(6): 1070-1077*.
13. Huisman TA (2009) Tumor-like lesions of the brain. *Cancer Imaging,* ***9****(Spec No A): S10-S13*.
14. Kobayashi M, Shimizu Y, Shibata N, Uchiyama S (2014) Gadolinium enhancement patterns of tumefactive demyelinating lesions: correlations with brain biopsy findings and pathophysiology. *J Neurol,* ***261****(10): 1902-1910*.
15. Cortese R, Magnollay L, Tur C, Abdel-Aziz K, *et al.* (2018) Value of the central vein sign at 3T to differentiate MS from seropositive NMOSD. *Neurology,* ***90****(14): e1183-e1190*.
16. Sharma R, Fischer MT, Bauer J, Felts PA, *et al.* (2010) Inflammation induced by innate immunity in the central nervous system leads to primary astrocyte dysfunction followed by demyelination. *Acta Neuropathol,* ***120****(2): 223-236*.
17. Bolcaen J, Acou M, Mertens K, Hallaert G, *et al.* (2013) Structural and metabolic features of two different variants of multiple sclerosis: a PET/MRI study. *J Neuroimaging,* ***23****(3): 431-436*.
18. Jain R, Ellika S, Lehman NL, Scarpace L, *et al.* (2010) Can permeability measurements add to blood volume measurements in differentiating tumefactive demyelinating lesions from high grade gliomas using perfusion CT? *J Neurooncol,* ***97****(3): 383-388*.

[Downloaded from ijrr.com on 2026-11-08]

[DOI: 10.61186/ijrr.24.4.11]

[DOI: 10.61186/ijrr.24.4.11] [Downloaded from ijrr.com on 2026-11-08]